

Ablation of vitreous tissue with a high repetition rate erbium:YAG laser

M.H.J. KRAUSE^{1,2}, D.J. D'AMICO¹

¹Retina Service and Laser Research Laboratory, Massachusetts Eye and Ear Infirmary, Department of Ophthalmology, Harvard Medical School, Boston, MA - USA

²Department of Ophthalmology and Eye Hospital, University of Saarland, Homburg (Saar) - Germany

PURPOSE. To quantify erbium (Er):YAG laser ablation of vitreous in relation to different pulse repetition rates 200 Hz, in order to examine the feasibility of laser for removal of vitreous gel (photovitreotomy) in clinically acceptable times.

METHODS. Fresh porcine vitreous samples and saline controls were ablated in air with an Er:YAG laser connected to a sapphire fiber at pulse energies between 1.0 and 21.2 mJ and at pulse repetition rates between 10 and 200 Hz. Net ablation rates were determined by weight measurement.

RESULTS. Reproducible and constant ablation rates were found for given laser parameters. Net ablation rates increased linearly with pulse repetition rate and nonlinearly with pulse energy. Expanded laser parameter domains permitted vitreous ablation rates as low as 1 µg/s to as high as 1031 µg/s. Ablation rates did not differ significantly between vitreous and saline.

CONCLUSIONS. The study documents clinically useful vitreous ablation rates that scale linearly with high repetition rates of Er:YAG laser, and suggests directions for further development of laser technology for enhanced removal of vitreous and other tissues. However, nonlinear effects of pulse energy also exist, indicating need for careful examination of ablation characteristics in various instruments. (Eur J Ophthalmol 2003; 13: 424-32)

KEY WORDS. Laser surgery—methods, Lasers—therapeutic use, Vitrectomy methods, Vitreous body surgery, Vitreous body—radiation effects

Accepted: March 12, 2003

INTRODUCTION

Erbium (Er):YAG laser radiation at 2.94 µm is highly absorbed by water and tissue. A variety of studies have demonstrated that the short penetration depth of Er:YAG laser allows precise cutting and ablation in numerous vitreoretinal surgical maneuvers (1-4). However, previous experimental and clinical studies documented limitations imposed by slow ablation rates with earlier laser systems. In contrast, the availability of a prototype high repetition (up to 200 Hz) Er:YAG laser permits a refined examination of the interaction

of pulse rate and energy in vitreous and other ocular tissues. Modeling and qualitative experimental data indicate that the use of high pulse repetition rates with lower energy minimizes mechanical injury and preserves efficient ablation (5-7). Furthermore, the new pulse energy and repetition rate domains suggest that the vitreous itself may be removed by laser ablation within surgically acceptable times (8), a process termed photovitreotomy (9). Similarly, a better understanding of the ablation dynamics of vitreous gel and saline will enhance the precision of laser ablation in more complex tissues encountered within the eye. Howev-

er, quantitative data on fluid and vitreous ablation are still limited (10), and with respect to the design of new vitreoretinal laser instruments, questions have been raised about optimal parameters with respect to efficacy and predictability of Er:YAG laser ablation. The purpose of this study was to quantify Er:YAG laser ablation of vitreous tissue and sodium chloride solution in dependence to different pulse energies and pulse repetition rates up to 200 Hz.

METHODS

Er:YAG laser and fiber

A pulsed, solid-state Er:YAG laser emitting at 2.94 μm (VersaPulse Select Erbium; Coherent, Palo Alto, CA, USA) was used for all experiments. The laser pulse duration was adjustable between 200 μs and 500 μs with incremental energy levels ranging from 1.0 mJ to 27.5 mJ per pulse (power: 10 mW to 5500 mW; measured as described below). Immediately before starting each series of experiments at constant laser parameters, the power was measured at the tip of our fiber by using a thermal laser head (LM-10; Coherent Auburn Group, Auburn, CA, USA) connected to a powermeter (Laser VP Select; Coherent). The repetition rate could be adjusted between 10 Hz and 200 Hz. The laser system was activated by a foot switch and incorporated a red diode-aiming beam to facilitate targeting of laser energy. The laser output was connected to a high-transmission mid-infrared fiber made of single crystal sapphire surrounded by a PTFE buffer (Saphikon, Inc., Milford, NH) (length: 1.5 m, fiber core diameter: 425 μm , effective numeric aperture: 0.12, Fresnel adjusted transmission per meter: 80%; data provided by the manufacturer). The laser power chosen for the experiment ranged between 54 mW and 4160 mW. Pulse energies between 1.0 and 21.2 mJ and pulse repetition rates of 10, 20, 30, 40, 50, 100, 150, and 200 Hz were used. The pulse duration was 500 μs for all experiments.

Preparation of vitreous tissue

Fresh porcine eyes were obtained from a local abattoir and immediately stored in physiologic sodium chloride solution at a temperature of +6 °C. The eyes were

prepared by creating a 360° incision 5 mm posterior and parallel to the limbus using a surgical blade and scissors. The anterior part of the eye, including the ciliary body and the vitreous attached to the posterior lens capsule, was carefully lifted with forceps. The lowest part of the vitreous was always cut off with a scissors as it usually contained pigment from the retinal pigment epithelial layer. The clear core part of the vitreous still attached to the posterior capsule was cut off and immediately transferred into test tubes while leaving the rest of the vitreous attached to the anterior segment. This standardized procedure was chosen to ensure that the core of vitreous gel was removed in all eyes. No liquid drops were observed on the surface of the vitreous gel.

Ablation measurements

Er:YAG laser ablation of vitreous was compared with ablation of sodium chloride solution (Abbot Laboratories, North Chicago, IL, USA) to isolate possible effects related to specific properties of vitreous. The sodium chloride solution contained 900 mg sodium chloride dissolved in 100 ml distilled water (154 mEq of sodium and 154 mEq of chloride; 308 mOsm/liter; pH 5.6). The net ablation rates of vitreous tissue as well as sodium chloride solution were determined by weight measurement (10). The weights of both substances were measured before and after laser treatment using precision scales (Mettler AE 200; Mettler Instrument Corp., Hightstown, NJ, USA) (range 0-200 g; precision 0.1 mg). Untreated control samples of vitreous and sodium chloride solution were used simultaneously to correct for evaporation. Net ablation rates were considered as the difference in the amounts of weight loss measured with and without laser treatment. Every individual treatment and control sample was weighed before and after treatment according to standardized time intervals (Tab. I). The duration of the treatment was 90 seconds. Each series of laser pulses was performed three times at constant experimental settings to minimize random error. In all series the sample volume was filled into polystyrene spectrophotometer cuvetts (Sigma-Aldrich Chemie GmbH, Steinheim, Germany).

Noncontact ablation was preferred to placing a laser fiber tip beneath the surface of the sample to avoid recondensation interfering with the measurement of

TABLE I - TIME COURSE OF ABLATION MEASUREMENTS

Time from start point, s	Procedure
0	Weight measurement of treatment sample
60	Weight measurement of control sample
90	Start of laser treatment
180	Stop of laser treatment
210	Weight measurement of treatment sample
270	Weight measurement of control sample

ablation. The tip of the fiber was mounted vertically above the center of the sample. A precision dial caliper was used to verify that the distance between the tip of the probe and the surface of the sample was constant at 3.8 mm, a distance that eliminated debris accumulation from spattering during ablation. New samples were provided immediately before starting each series of ablation measurements at new laser settings. The room temperature in the laboratory was 22 ± 2 °C. The water content in the air was permanently measured with a hygrometer and maintained at 55% with variation less than $\pm 2\%$.

Statistics

The initial hypothesis (H0) to be determined was that there were no significant differences between ablation of sodium chloride and vitreous, respectively. Data

were expressed as mean \pm standard deviation. The Mann-Whitney U-test was used to assess the significance of differences in ablation rates of sodium chloride and vitreous. A probability value <0.05 was considered statistically significant.

RESULTS

Constant ablation rates were found for both vitreous and sodium chloride solution in each of three consecutive series at constant laser parameters. For most measurements, the standard deviation was within 15% of the total amount of ablated weight (Tabs. II, III). Ablation rates per second ranged from 1 μg to 1031 μg in vitreous (Tab. II) and from 7 μg to 1107 μg in sodium chloride solution (Tab. III). There was an insignificant trend toward higher ablation rates in sodium chloride solution compared to vitreous tissue ($p=0.25$).

For all pulse frequencies tested, the net ablation rates per second in both vitreous tissue and sodium chloride solution exhibited a linear increase with increasing pulse frequency (Figs. 1, 2). However, a non-linear increase of net ablation rates per second with increasing pulse energies was detected in vitreous and sodium chloride solution (Figs. 3, 4). A scatter diagram (Fig. 5) shows the net ablation rates of vitreous per second divided through the power of the laser light (y-axis) in dependence to the power of the laser light (x-axis). The relative amount of ablation in-

TABLE II - NET ABLATION RATES OF VITREOUS PER SECOND AT DIFFERENT PULSE ENERGIES AND REPETITION RATES

Pulse energy, mJ	Pulse repetition rate, Hz							
	10	20	30	40	50	100	150	200
1.06 \pm 0.02					1 \pm 1	16 \pm 1	17 \pm 1	18 \pm 2
2.22 \pm 0.05					4 \pm 0	11 \pm 6	21 \pm 3	30 \pm 0
4.62 \pm 0.15	2 \pm 1	4 \pm 0	7 \pm 1	11 \pm 1	13 \pm 1	38 \pm 6	69 \pm 6	109 \pm 3
8.11 \pm 0.19	3 \pm 2	24 \pm 1	29 \pm 4	32 \pm 2	60 \pm 9	182 \pm 16	266 \pm 8	379 \pm 19
10.62 \pm 0.71	9 \pm 1	24 \pm 3	44 \pm 1	64 \pm 3	63 \pm 3	251 \pm 14	324 \pm 24	441 \pm 23
15.97 \pm 0.23	27 \pm 4	53 \pm 2	80 \pm 6	116 \pm 8	139 \pm 7	349 \pm 27	476 \pm 24	704 \pm 64
19.99 \pm 0.38	36 \pm 6	67 \pm 2	128 \pm 14	169 \pm 12	220 \pm 30	458 \pm 32	742 \pm 63	1031 \pm 92

Net ablation rates of vitreous per second ($\mu\text{g/s}$) are expressed as average \pm SD, and calculated from three measurements at constant laser parameters. The left column of the table contains average pulse energies (mJ) calculated from power measurements (see Methods)

TABLE III - NET ABLATION RATES OF SODIUM CHLORIDE SOLUTION PER SECOND AT DIFFERENT PULSE ENERGIES AND REPETITION RATES

Pulse energy, mJ	Pulse frequency, Hz							
	10	20	30	40	50	100	150	200
1.05 ± 0.03					7 ± 3	12 ± 1	19 ± 0	27 ± 0
2.06 ± 0.07					13 ± 1	22 ± 0	41 ± 1	60 ± 2
4.54 ± 0.22	11 ± 1	12 ± 1	22 ± 3	30 ± 2	30 ± 3	52 ± 3	91 ± 3	143 ± 2
7.67 ± 0.24	14 ± 2	26 ± 2	36 ± 0	51 ± 3	81 ± 4	179 ± 9	264 ± 22	407 ± 7
10.12 ± 0.32	23 ± 3	37 ± 1	64 ± 2	91 ± 2	112 ± 3	257 ± 10	406 ± 26	543 ± 30
15.67 ± 0.48	33 ± 1	68 ± 1	110 ± 4	158 ± 3	188 ± 6	408 ± 17	669 ± 24	879 ± 54
20.59 ± 0.43	34 ± 2	86 ± 2	134 ± 4	178 ± 9	246 ± 8	581 ± 44	899 ± 30	1107 ± 16

Net ablation rates of sodium chloride solution per second ($\mu\text{g/s}$) are expressed as average \pm SD, and calculated from three measurements at constant laser parameters. The left column of the table contains average pulse energies (mJ) calculated from power measurements (see Methods)

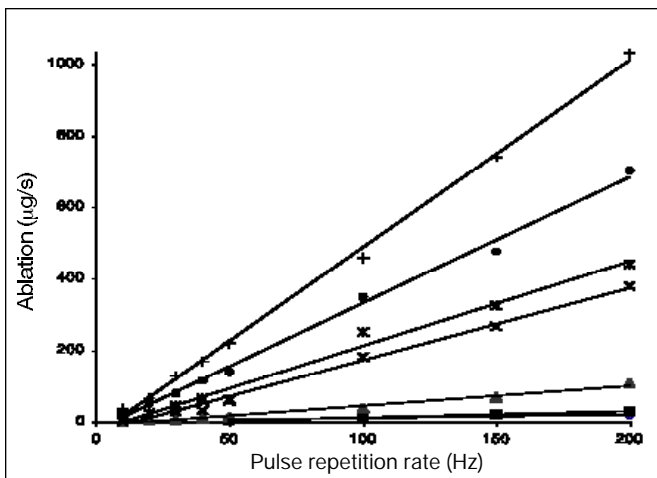


Fig. 1 - Net ablation rates of vitreous tissue per second ($\mu\text{g/s}$) in dependence to pulse repetition rates (Hz). For all pulse energies (mJ), the net ablation rates show a linear increase with increasing pulse repetition rates.

◆ = 1.06 ± 0.02 mJ; ■ = 2.22 ± 0.05 mJ; ▲ = 4.62 ± 0.15 mJ;
 X = 8.11 ± 0.19 mJ; * = 10.62 ± 0.71 mJ; ● = 15.97 ± 0.23 mJ;
 + = 19.99 ± 0.38 mJ.

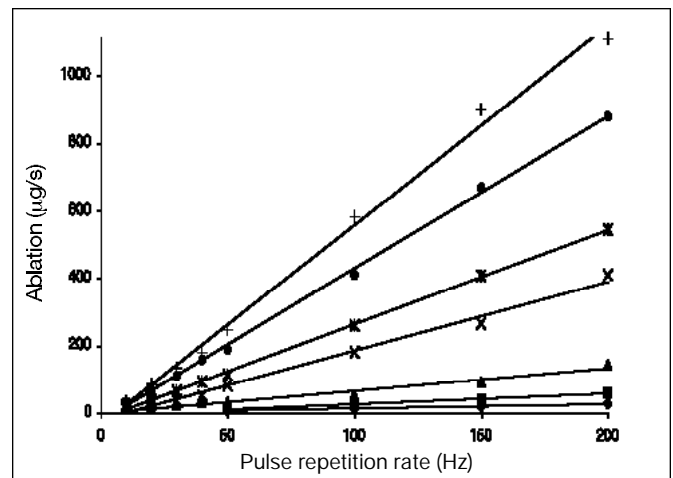


Fig. 2 - Net ablation rates of sodium chloride solution per second ($\mu\text{g/s}$) in dependence to pulse repetition rates (Hz). For all pulse energies (mJ), the net ablation rates show a linear increase with increasing pulse repetition rates.

◆ = 1.05 ± 0.03 mJ; ■ = 2.06 ± 0.07 mJ; ▲ = 4.54 ± 0.22 mJ;
 X = 7.67 ± 0.24 mJ; * = 10.12 ± 0.32 mJ; ● = 15.67 ± 0.48 mJ;
 + = 20.59 ± 0.43 mJ.

creased with increasing power of the laser light up to about 1000 mW and remained constant above about 1000 mW. The fluctuation of the relative ablation decreased with increasing power. An analogue scatter diagram for sodium chloride solution (Fig.6) revealed similar results. The relative amount of ablation increased with increasing power of the laser light up to about 1500 mW and remained constant above this power.

DISCUSSION

Although initially attractive to vitreoretinal surgeons as a potential tool for high precision and tractionless cutting of abnormal tissues within the eye, the Er:YAG laser is increasingly explored as a technology to remove the vitreous gel itself, in a process known as photovitrectomy. The potential of the Er:YAG laser to

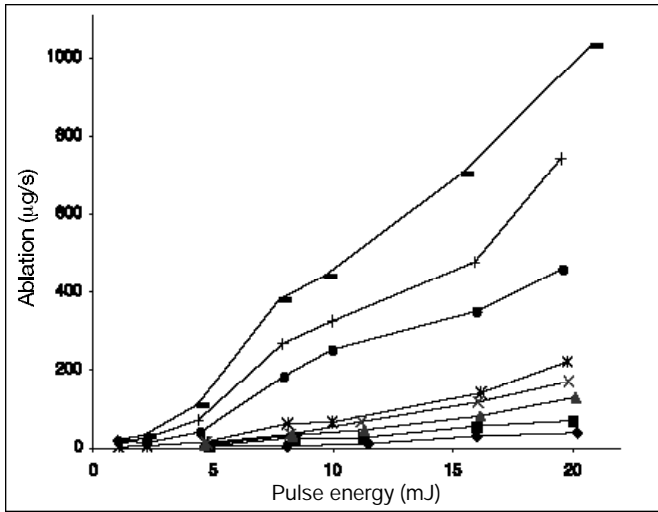


Fig. 3 - Net ablation rates of vitreous tissue per second ($\mu\text{g/s}$) in dependence to pulse energy (mJ). For all pulse frequencies (Hz), the net ablation rates show a linear increase with increasing pulse energy. \blacklozenge = 10 Hz; \blacksquare = 20 Hz; \blacktriangle = 30 Hz; \times = 40 Hz; $*$ = 50 Hz; \bullet = 100 Hz; $+$ = 150 Hz; $-$ = 200 Hz.

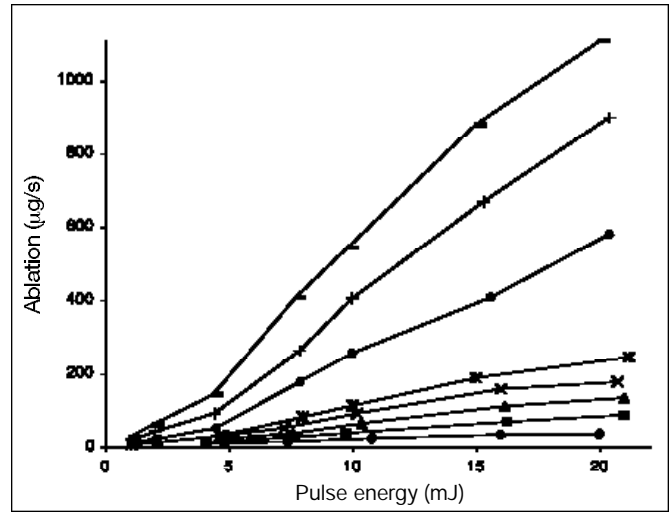


Fig. 4 - Net ablation rates of sodium chloride solution per second ($\mu\text{g/s}$) in dependence to pulse energy (mJ). For all pulse frequencies (Hz), the net ablation rates show a linear increase with increasing pulse energy. \blacklozenge = 10 Hz; \blacksquare = 20 Hz; \blacktriangle = 30 Hz; \times = 40 Hz; $*$ = 50 Hz; \bullet = 100 Hz; $+$ = 150 Hz; $-$ = 200 Hz.

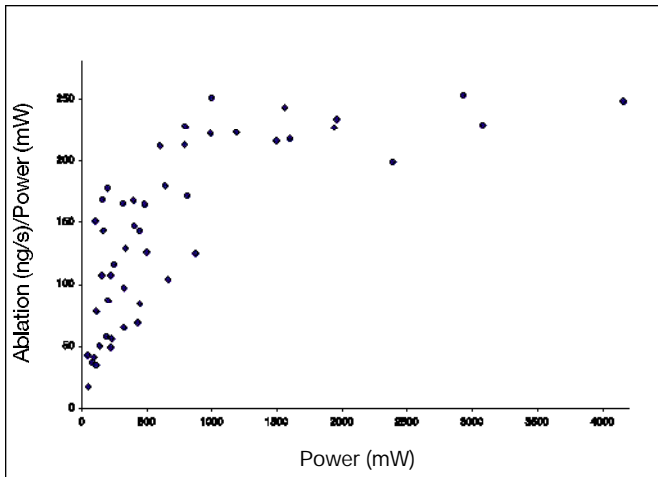


Fig. 5 - Scatter diagram of net ablation rates of vitreous divided through the duration of the laser ablation and the power of the laser light ($\text{ng/s} \times \text{mW}$) in dependence to the power of the laser light (mW). Below 1000 mW, the relative ablation increases with increasing power of the laser light, while it remains high above 1000 mW. The fluctuation of the relative ablation decreases with increasing power.

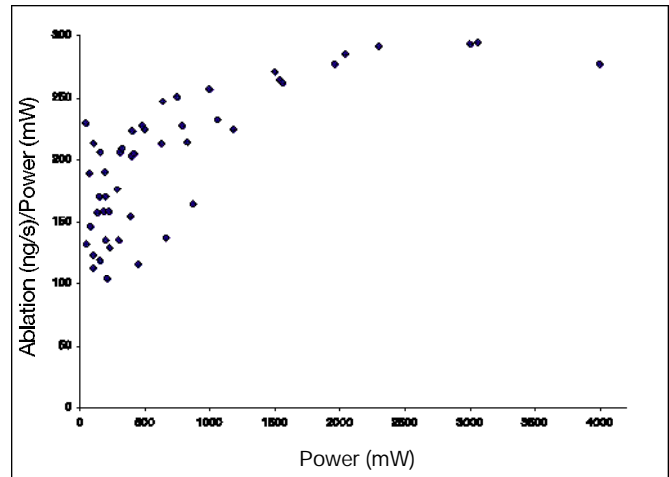


Fig. 6 - Scatter diagram of net ablation rates of sodium chloride solution divided through the duration of the laser ablation and the power of the laser light ($\text{ng/s} \times \text{mW}$) in dependence to the power of the laser light (mW). Below 1000 mW, the relative ablation increases with increasing power of the laser light, while it remains high above 1500 mW. The fluctuation of the relative ablation decreases with increasing power.

perform diverse maneuvers in vitreoretinal surgery and emulate hand-held instruments such as blades, forceps, scissors, and vitreous cutters is dependent on its fundamental absorption by tissue water and modified by many parameters including repetition rate,

pulse energy, pulse duration, and delivery system geometry. The present study documents the effects of high repetition rates and variable pulse energies on the ablation rate of vitreous, and suggests that the Er:YAG laser integrated in an irrigation – aspiration – device

can be developed as an instrument to remove vitreous in surgically acceptable times. In a clinical study using irrigation and aspiration, the mean cutting time was 420 ± 152 seconds for the laser vitrectomy group compared to 301 ± 120 seconds for the mechanical vitrectomy group (8). Furthermore, although nonlinear effects of pulse energy were also noted in this study, the expanded repetition rate and pulse energy domains available in the prototype laser provide a finer gradation of ablation that will enhance the precision of laser energy application in vitrectomy as well as in other maneuvers of interest to vitreoretinal surgeons, such as membrane cutting.

At constant pulse duration, the fluence, pulse energy, and pulse repetition rate are considered to be variables most important for intended tissue ablation and tissue dissection as well as unintended tissue damage. Bubble formation resulting from explosive vaporization and optical breakdown with plasma formation mediates tissue injury by complex thermal and mechanical mechanisms, e.g., emission of shock waves. Linear proportionality exists for pulse energy and vapor bubble volume, as well as for pulse energy and collapse pressure (6, 11-14). For Q-switched laser operation, pressure transients at bubble expansion and bubble collapse show comparable altitudes up to several hundreds of bars. For free-running laser operation the pressure transients induced by the bubble collapse are an order of magnitude stronger than the pressure waves resulting from the explosive ablation process caused by each individual laser spike (12). Whereas tissue damage from mechanical and thermal effects mainly depends on the total deposited energy, ablation depth and tissue transection are likely to be determined by radiant exposure (J/cm^2) (6, 14). Recent clinical studies have therefore used pulse energies far below 20 mJ (4, 8). Our study shows that the amount of ablation can be preserved at lower laser pulse energies if the pulse repetition rate is increased accordingly. In considering fiberoptic applications, smaller probe tips offer lower pulse energies while maintaining the amount of fluence, and therefore optimize the ablative capabilities with respect to the potential for untoward tissue injury (6).

A particular challenge exists when unshielded laser fibers without irrigation and aspiration are used to ablate large amounts of vitreous in a closed system such as the eye. An experimental study measured temperature

increases between 8 and 16.5 °C in pig eyes for a pulse repetition rate of 20 Hz and a pulse energy of 15 mJ (15). However, the increase in temperature is much smaller in clinical settings, where appropriately designed endoprobes reduce the acoustomechanical effects of laser ablation and where irrigation and aspiration reduce heat accumulation (16, 17). Also, appropriately designed endoprobes should reduce the acoustomechanical effects of laser ablation.

Modeling studies have suggested the use of higher repetition rates and these findings have been supported recently, when prototypes of Er:YAG lasers with higher repetition rates became available for pre-clinical (7) and clinical (4) procedures. At constant probe parameters, theoretical considerations for laser-generated bubble expansion suggest that high repetition rates up to 1000 Hz should merely accelerate tissue removal, without fundamentally altering the laser-tissue interaction (6). These conclusions were based on the bubble reverberations observed by optical, acoustic, and high-speed photographic techniques. The reverberations were essentially complete 1 ms after initiation of irradiation (18-20). Furthermore, temperature increases measured 500 μ m from the laser tip in experimental studies (bovine vitreous) and model systems were found to depend on the pulse energy rather than the pulse repetition rate (5). Recently, Brazitikos et al tested a high repetition rate Er:YAG laser in vivo. Qualitative observations of vitreoretinal procedures and damaging zones in histopathologic specimens indicated that the use of high pulse repetition rates with lower energy may actually minimize thermomechanical injury and preserve efficient ablation (7). The quantitative experimental findings of our work are in agreement with these modeling and experimental studies. For all pulse energies tested the net ablation rates per second both in vitreous tissue and sodium chloride solution exhibited a linear increase with increasing pulse repetition rates (Figs. 1, 2).

For all repetition rates studied, the ablation rates of both vitreous and sodium chloride solution increased nonlinearly with an increasing pulse energy (Figs. 3, 4). With reference to Walsh et al, an attempt was made to match the data with a simple dynamic model for ablation by plotting the amount of ablation vs. the logarithm of the incident pulse energy (21, 22), but the amount of ablation was found not to be linearly

dependent on the logarithm of pulse energy. Figures 5 and 6 quantify the efficacy of ablation, i.e., the amount of ablation relative to the power, for a variety of different repetition rates and pulse energies. A higher and constant efficacy of ablation as well as lower fluctuation indicating a better predictability was detected for a power above 1000 mW to 1500 mW. This change of efficacy and predictability of ablation rates can be explained by the nonlinear dependence on the pulse energy mentioned above. Thermal and mechanical modeling studies may aid in the understanding of the nonlinear relationship, although a detailed discussion of individual models is beyond the scope of this work. The ablation of tissue by 2.94 μm radiation is an explosive process driven by rapid heating and thermal expansion, electrostrictive stress, explosive vaporization, and optical breakdown with plasma production. Unlike Beer's law blow-off model dynamic models consider removal of material during the pulse with ablation depths in the range of several millimeters (6, 23-25). High-temperature, high-pressure gases develop at the site of absorption, which are capable of breaking bonds in tissue (25). Ablated material can leave the surface at supersonic velocities and expose deeper tissue or is pushed against the walls of the crater (21, 24, 26, 27). Furthermore, the absorption at 2.94 μm decreases substantially in vaporized water and therefore much deeper penetration is possible. Statistical models suggest that in vaporized water at 100 atmospheres, 3,000 °K, the absorption coefficient, μ_a , is approximately 2.7 cm^{-1} , compared to approximately 13,000 cm^{-1} in liquid water at room temperature (25, 28). Each of the factors mentioned may have contributed to the nonlinear and nonlogarithmic relationship between ablated material and pulse energy. The potential for collateral tissue damage by decreased absorption of 2.94 μm in vapor further supports the goal of minimizing pulse energy and protecting collateral tissues by appropriate endoprobe geometries. Based on the complex thermomechanical interactions, it is not surprising that methodologic differences between ablation studies led to substantial differences in their results (21, 24, 29-33). A survey of further studies evaluating laser ablation of different tissues is given by Hibst (29). Several studies found a linear increase of ablation with increasing pulse energy (24, 29, 30, 32). Higher fluences than those in the present study were

reported to correlate linearly with the ablation rate of vitreous and sodium chloride solution (10). Other studies detected an increasing efficacy, i.e., a non-linear increase of ablation, with increasing fluences (21, 31, 33).

Comparison of ablation of sodium chloride solution and vitreous revealed a similar amount of ablation as well as similar mathematical relationships between the parameters studied. A slightly lower ablation rate of vitreous, although not statistically significant in this study, may exist (10) and can be explained by the evaporation enthalpy of soluble vitreous proteins exceeding the amount necessary for evaporation of water. Furthermore, the ultrastructural organization of the vitreous (34, 35) may affect the thermal laser tissue interaction as discussed elsewhere (10).

The extraordinary precision needed in intraocular surgery of the retina and vitreous requires the use of increasingly refined techniques for tissue manipulation and removal if improved clinical results are to be attained. The present studies suggest directions for the development of instrumentation for enhanced removal of vitreous and other tissues. These directions include instruments with a higher number of laser pulses per second (above 200) as well as the study of appropriately designed endoprobe geometries.

Validation is necessary in a more complex clinical environment, with additional parameters to be considered, such as irrigation and aspiration. Future experiments will explore vitreous removal and intraocular tissue ablation and cutting with instrumentation guided by the presently described parameters.

ACKNOWLEDGEMENTS

Supported by Vitreoretinal Research Fund, DFG Kr 1918/1, DFG Kr 1918/2.

Reprint requests to:
Matthias H.J. Krause, MD
Department of Ophthalmology
University of Saarland
Kirrberger Strasse 1
66424 Homburg (Saar), Germany
mhj_krause@web.de

REFERENCES

1. D'Amico DJ, Moulton RS, Theodosiadis PG, Yarborough JM. Erbium:YAG laser photothermal retinal ablation in enucleated rabbit eyes. *Am J Ophthalmol* 1994; 117: 783-90.
2. Brazitikos PD, D'Amico DJ, Bernal MT, Walsh AW. Erbium:YAG laser surgery of the vitreous and retina. *Ophthalmology* 1995; 102: 278-90.
3. D'Amico DJ, Brazitikos PD, Marcellino GR, Finn SM, Hobart JL. Initial clinical experience with an erbium:YAG laser for vitreoretinal surgery. *Am J Ophthalmol* 1996; 121: 414-25.
4. D'Amico DJ, Blumenkranz MS, Lavin MJ, et al. Multicenter clinical experience using an erbium:YAG laser for vitreoretinal surgery. *Ophthalmology* 1996; 103: 1575-85.
5. Berger JW, Bochow TW, Talamo JH, D'Amico DJ. Measurement and modeling of thermal transients during Er:YAG laser irradiation of vitreous. *Lasers Surg Med* 1996; 19: 388-96.
6. Berger JW, D'Amico DJ. Modeling of erbium:YAG laser-mediated explosive photovaporization: implications for vitreoretinal surgery. *Ophthalmic Surg Lasers* 1997; 28: 133-9.
7. Brazitikos PD, D'Amico DJ, Bochow TW, Hmelar M, Marcellino GR, Stangos NT. Experimental ocular surgery with a high-repetition-rate erbium:YAG laser. *Invest Ophthalmol Vis Sci* 1998; 39: 1667-75.
8. Petersen H, Mrochen M, Seiler T. Comparison of erbium:yttrium-aluminum-garnet-laser vitrectomy and mechanical vitrectomy: a clinical study. *Ophthalmology* 2000; 107: 1389-92.
9. Bochow TW, Kim RY, Berger JW, D'Amico DJ. Photovitreotomy-a novel approach for vitreous removal. *Invest Ophthalmol Vis Sci* 1995; 36: S384.
10. Krause M, Steeb D, Foth HJ, Weindler J, Ruprecht KW. Ablation of vitreous tissue with erbium:YAG laser. *Invest Ophthalmol Vis Sci* 1999; 40: 1025-32.
11. Frenz M, Pratisto H, Ith M, Konz F, Weber HP. Effects of simultaneously fiber transmitted Erbium and Holmium radiation on the interaction with highly absorbing media. *Proc SPIE* 1995; 2391: 517-24.
12. Frenz M, Pratisto H, Ith M, et al. Transient photoacoustic effects induced in liquids by pulsed erbium lasers. *Proc SPIE* 1994; 2134A: 402-11.
13. Asshauer T, Rink K, Delacretaz G, et al. Acoustic transient generation in pulsed holmium laser ablation underwater. *Proc SPIE* 1994; 2134A: 423-33.
14. Berger JW, Bochow TW, Kim RY, D'Amico DJ. Biophysical considerations for optimizing energy delivery during Er:YAG laser vitreoretinal surgery. *Proc SPIE* 1996; 2673: 146-56.
15. Wilkens V, Wiemann C, Koch C, Foth H-J. Fiber-optic dielectric multilayer temperature sensor: in situ measurement in vitreous during Er:YAG laser irradiation. *Optics Laser Technology* 1999; 31: 593-9.
16. Mrochen M, Petersen H, Wullner C, Seiler T. Experimentelle Ergebnisse zur Erbium: YAG-Laservitrektomie. *Klin Monatsbl Augenheilkd* 1998; 212: 50-4.
17. Mrochen M, Riedel P, Kempe A, Seiler T. Erbium:YAG-Laservitrektomie: Temperaturmessungen in unterschiedlichen Austauschmedien. *Ophthalmologie* 2000; 97: 181-5.
18. Lin CP, Weaver YK, Birngruber R, Fujimoto JG, Puli-afito CA. Intraocular microsurgery with a picosecond Nd:YAG laser. *Lasers Surg Med* 1994; 15: 44-53.
19. Loertscher H, Shi WQ, Grundfest WS. Tissue ablation through water with erbium:YAG lasers. *IEEE Trans Biomed Eng* 1992; 39: 86-8.
20. Brinkmann R, Droge G, Schroer F, Scheu M, Birngruber R. Ablation dynamics in laser sclerostomy Ab externo by means of pulsed lasers in the mid-infrared spectral range. *Ophthalmic Surg Lasers* 1997; 28: 853-65.
21. Walsh JT Jr., Deutsch TF. Er:YAG laser ablation of tissue: measurement of ablation rates. *Lasers Surg Med* 1989; 9: 327-37.
22. Walsh JT, Jr., Deutsch TF. Pulsed CO₂ laser tissue ablation: measurement of the ablation rate. *Lasers Surg Med* 1988; 8: 264-75.
23. Berger JW. Erbium-YAG laser ablation: the myth of 1- μ m penetration. *Arch Ophthalmol* 1998; 116: 830.
24. Zweig AD, Frenz M, Romano V, Weber HP. A comparative study of laser tissue interaction at 2.94 μ m and 10.6 μ m. *Appl Phys B* 1988; 47: 259-65.
25. Walsh JT, Jr., Flotte TJ, Deutsch TF. Er:YAG laser ablation of tissue: effect of pulse duration and tissue type on thermal damage. *Lasers Surg Med* 1989; 9: 314-26.
26. Walsh JT. Pulsed laser ablation of tissue: analysis of the removal process and tissue healing [dissertation]. Boston: MIT; 1988.
27. Zweig AD, Weber HP. Mechanical and thermal parameters in pulsed laser cutting of tissue. *IEEE J Quantum Electron* 1987; 23: 1787-92.
28. Young JS. Evaluation of nonisothermal band model for H₂O. *J Quant Spectrosc Radiat Transfer* 1977; 18: 29-45.
29. Hibst R. Technik, Wirkungsweise und medizinische Anwendungen von Holmium- und Erbium-Lasern. Landsberg: Ecomed-Verlag, 1996; 46-66.
30. Gaillitis RP, Patterson SW, Samuels MA, Hagen K, Ren Q, Waring GO. Comparison of laser phacovaporization using the Er-YAG and the Er-YSGG laser. *Arch Ophthalmol* 1993; 111: 697-700.
31. Ross BS, Puli-afito CA. Erbium-YAG and holmium-YAG laser ablation of the lens. *Lasers Surg Med* 1994; 15: 74-82.

32. Hohenleutner U, Hohenleutner S, Baumler W, Landthaler M. Fast and effective skin ablation with an Er:YAG laser: determination of ablation rates and thermal damage zones. *Lasers Surg Med* 1997; 20: 242-7.
33. Jean B, Bende T. Photoablation of gelatin with the free-electron laser between 2.7 and 6.7 microns. *J Refract Corneal Surg* 1994; 10: 433-8.
34. Scott JE. Extracellular matrix, supramolecular organisation and shape. *J Anat* 1995; 187: 259-69.
35. Scott JE, Thomlinson AM. The structure of interfibrillar proteoglycan bridges ('shape modules') in extracellular matrix of fibrous connective tissues and their stability in various chemical environments. *J Anat* 1998; 192: 391-405.